Space Weather

RESEARCH ARTICLE
10.1029/2022SW003144

Potential Impact of GNSS Positioning Errors on the Satellite-Navigation-Based Air Traffic Management

Dabin Xue[1,2], Jian Yang[2], and Zhizhao Liu[1]

[1]Department of Land Surveying and Geo-Informatics, The Hong Kong Polytechnic University, Hong Kong, China, [2]Department of Earth and Space Sciences, Southern University of Science and Technology, Shenzhen, China

Key Points:

- Satellite-navigation-based air traffic management (ATM) scenario is simulated to assess the potential impact of Global Navigation Satellite System positioning errors
- The rules for ATM during severe space weather events are presented
- Financial cost related to airlines can be 2 million Euros without ionospheric delay forecast for Hong Kong International Airport during a geomagnetic storm

Correspondence to:
J. Yang and Z. Liu,
yangj36@sustech.edu.cn;
lszzliu@polyu.edu.hk

Citation:
Xue, D., Yang, J., & Liu, Z. (2022). Potential impact of GNSS positioning errors on the satellite-navigation-based air traffic management. *Space Weather*, *20*, e2022SW003144. https://doi.org/10.1029/2022SW003144

Received 4 MAY 2022
Accepted 2 JUN 2022

Author Contributions:
Formal analysis: Dabin Xue
Methodology: Dabin Xue
Supervision: Jian Yang, Zhizhao Liu
Writing – original draft: Dabin Xue
Writing – review & editing: Jian Yang, Zhizhao Liu

Abstract The traditional air traffic management (ATM) is transforming to the Communication, Navigation, Surveillance/ATM, which relies on accurate Global Navigation Satellite System (GNSS) navigation service, particularly during the final approach and landing phases. However, in the event of adverse space weather, there may be a significant increase in total electron contents (TECs) and irregularities in the ionosphere, which may cause considerable GNSS positioning errors. As a result, the aircraft navigation mode has to be switched from satellite navigation to ground navigation, which will reduce the airport acceptance rate and cause an imbalance between flight demands and airport capacity. The ATM authority will have to make tactical measures to remedy the problem, such as flight rescheduling and even cancellations. Hong Kong International Airport (HKIA) is one of the busiest airports in the world and Hong Kong, located in the equatorial ionosphere anomaly region, is prone to impacts of space weather. Thus, we have created a hypothesis scenario in this study by analyzing projected flight data from the HKIA during a simulated geomagnetic storm. Calculation results show that without an ionospheric delay forecast, the potential financial costs related to airlines due to flight delays, cancellations, and diversions could be over 2 million Euros. These costs decrease with an increased lead time of ionospheric delay forecast and the inaccurate ionospheric delay forecast can also result in significant extra costs. We also estimate the time cost of flight delays to passengers can be between 1.7 and 3.0 million Euros.

Plain Language Summary During the final approach and landing phases, aircraft navigation now primarily relies on the ground facilities. To meet the growing need for civil aviation, the International Civil Aviation Organization promotes satellite navigation to increase airspace capacity and flight efficiency. As a result, aircraft will navigate using the Global Navigation Satellite System (GNSS). However, due to the considerable increase in total electron contents and irregularities in the ionosphere, GNSS positioning accuracy will be degraded significantly during severe space weather. This research aims to explore the impact of GNSS positioning errors on satellite-based air traffic management. For an intense geomagnetic storm event affecting the Hong Kong International Airport, our calculation results reveal that the financial costs could be about 2 million Euros related to airlines and up to 3 million Euros related to passengers.

1. Introduction

The growing flight demand exceeds the limited airspace capacity, causing severe flight congestion and costly delays (Bubalo & Gaggero, 2021). Therefore, to satisfy the predicted growth in air traffic demand, the current air traffic management (ATM) system will need to be upgraded (Xue et al., 2021). In response, the International Civil Aviation Organization (ICAO) has proposed the Communication, Navigation, Surveillance for ATM, aiming to increase airspace capacity and flight efficiency by reducing aircraft horizontal and vertical separation standards without compromising flight safety (Vismari & Junior, 2011). Accordingly, satellite-based navigation via the Global Navigation Satellite System (GNSS) will replace the traditional ground navigation system as the primary source for aircraft navigation (Blanch et al., 2012), as GNSS can provide more accurate lateral and vertical guidance during enroute, terminal, and approach phases. Satellite-navigation-based aircraft can even land on runway in poor meteorological conditions (Lee et al., 2016), and fly along any desired flight paths instead of the traditional less efficient routes between two ground-based radio navigation points (Enge et al., 2015). Therefore, runway and airspace capacity can be improved due to the highly accurate and reliable real-time, three-dimensional aircraft position. The schematic diagram of satellite-based ATM is shown in Figure 1.

Currently, GNSS can provide aircraft with positioning accuracy of 5–20 m in calm geomagnetic conditions, which is insufficient for aircraft landing (Sharma & Hablani, 2014). This is because GNSS satellite signals are

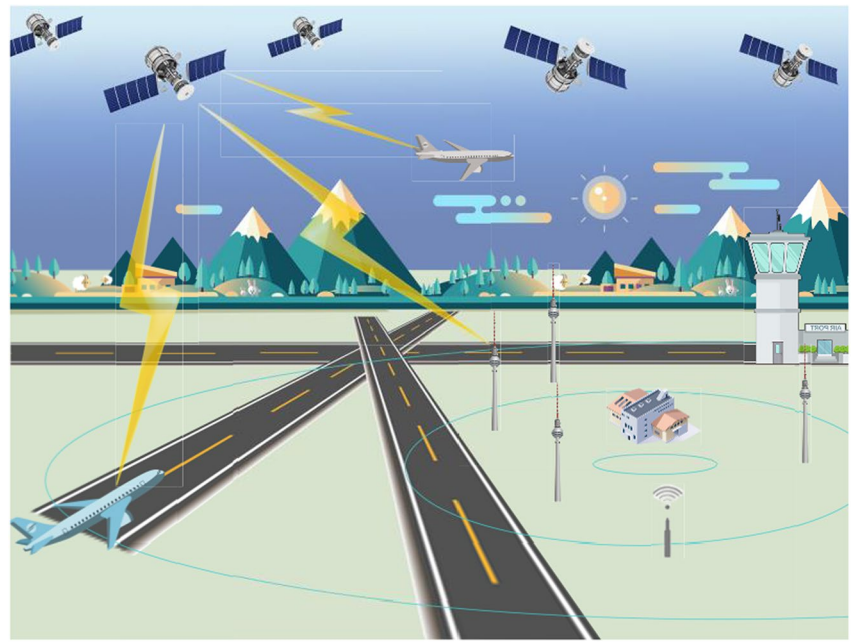

Figure 1. Schematic diagram of satellite-navigation-based air traffic management.

affected by a number of errors including satellite clock error (Guo & Geng, 2018), satellite orbit error (Zhang et al., 2019), tropospheric delay error (Ziv et al., 2021), receiver noise (J. Kim et al., 2019), multipath (Sun et al., 2019), and ionospheric error (Yu & Liu, 2021a, 2021b). Specifically, the positioning error caused by ionosphere is one of the most important factors and it is heavily affected by geomagnetic storms, one kind of the most intense space weather events. The electric field, neutral wind, and its composition in the ionosphere can be strongly disturbed during geomagnetic storms. The low-latitude ionosphere is especially vulnerable due to the equatorial plasma fountain effect (Tsurutani et al., 2004), which lifts the plasma to higher altitudes by an eastward electric field and generates enhanced ionization regions on the sides of the magnetic equator as the particles slide down along magnetic field lines. The Dst index is defined as the disturbed north-south component of geomagnetic field on Earth's surface in the low-latitude region. Geomagnetic storms with minimum Dst < -250 nT are usually denoted as super storms (Astafyeva et al., 2014). Several super storms occurred in the past such as those on 13 March 1989, 15 July 2000, and 29 October 2003 with the minima Dst $= -589$, -300, and -383 nT, respectively. According to (National Research Council, 2008), the storms in October 2003 had caused the vertical navigation guidance unavailable for aircraft precise approaching for a long time throughout most of the United States, leading to considerable societal and economic consequences.

The ionospheric correction for single-frequency GNSS receivers usually uses a thin shell model, which considers the three-dimensional ionosphere to condense on a two-dimensional thin shell (Huang & Yuan, 2013). The accuracy of positioning using the thin shell model is generally acceptable. However, during periods of considerable ionospheric disturbance, the thin shell model may be insufficient to describe the more complex three-dimensional fluctuations, resulting in decreased positioning accuracy and possible loss of integrity. GNSS positioning performance can be severely degraded during strong space weather periods, as illustrated in Table 1. Coster and Yizengaw (2021) summarize the effects of geomagnetic storms in three categories: (a) large gradients in ionospheric electron density can cause significant range errors and bending (Hoque & Jakowski, 2011); (b) even small-scale irregularities in the ionosphere can cause GNSS signal fluctuations (or scintillation) or even loss of lock; and (c) solar radio bursts can also cause notable effects on GNSS signals by raising the background noise level (Cerruti et al., 2008). Therefore, to reduce the degradation effects of space weather on ionosphere, the ionospheric total electron contents (TECs) forecast is vitally important (Cesaroni et al., 2020; Tsagouri et al., 2018).

Because the ground navigation systems such as the Instrument Landing System (ILS) are widely utilized around the world to provide accurate lateral and vertical approach guidance (E. Kim & Choi, 2016), flights have never officially suffered a landing failure despite low GNSS positioning performance in space weather circumstances.

Table 1
Cases of Large Global Navigation Satellite System (GNSS) Positioning Errors Caused by Space Weather Events

Time	Geographical location	Condition	Minimum Dst	Positioning errors	Source
7 to 8 September 2017	78.2°N and 16.0°E	Intense geomagnetic condition	−122 nT	Increase from 2 to 6 m at Longyearbyen, Norway	Linty et al. (2018)
September 2002 to April 2003	13.7°N and 100.8°E	S_4 (~0.6)	−181 nT	Exceed 10 m at KMLT, Thailand	Phoomchusak et al. (2013)
January to December 2001	19.6°N and 99.5°E	S_4 (>0.7)	−387 nT	Reach 14 m in longitude and 22 m in latitude at Chiang Rai, Thailand	Dubey et al. (2006)
April 2004	3.0°S and 40.2°E	Severe ionospheric scintillation	−117 nT	Reach 4 m in vertical components at Malindi, Kenya	Moreno et al. (2011)

Note. The S_4 index is derived from the detrended signal intensities of GNSS signals.

However, ATM is transitioning from ground-based navigation to satellite-based navigation to meet the expected growth of flight demands. It is clear that satellite-based navigation will become more common in the future. If a severe geomagnetic storm occurs, GNSS positioning errors will increase due to the increased ionospheric impacts, particularly in the low-altitude regions. As a result, aircraft cannot perform safe approach or landing solely based on satellite navigation, causing flight delays, flight diversions, and flight cancellations (Pejovic et al., 2009). To the best of our knowledge, very few studies have incorporated multiple factors such as space weather, GNSS positioning errors, and ATM into consideration. Hong Kong International Airport (HKIA) is one of the busiest airports in the world and Hong Kong is located in the Equatorial Ionization Anomaly region (Lin et al., 2007). This implies that HKIA is expected to suffer larger impacts from severe space weather events. Combining the upcoming flight demand and a hypothetic geomagnetic storm, we conduct a forward-looking analysis to assess the potential impact of GNSS positioning errors on ATM. This study is anticipated to provide valuable information and strategic recommendations for the aviation industry to handle the future space weather impacts.

2. Scenario Assumptions and Air Traffic Management Methodology

Our study is to investigate the potential impact of GNSS positioning errors induced by space weather on upcoming ATM, thus some priori information and scenario assumptions are required. The impact of the ionospheric delay on GNSS positioning errors is simplified in Section 2.1. The scenario assumptions are described in Section 2.2. The specific ATM rules and the solution methodology for ATM during space weather events are presented in Sections 2.3 and 2.4, respectively.

2.1. Temporal Ionospheric Delay

As shown in Figure 2a, a two-dip intense geomagnetic storm occurred on 8–11 September 2017, with the minima Dst = −122 nT at Hong Kong local time (LT) 10:00 on 8 September and −109 nT at 01:00 LT on 9 September. Figure 2b shows that there was a sharp increase in the ionospheric TEC toward ~12:00 LT. The ionospheric delay τ (in the units of meters) is proportional to the TEC, and can be calculated using $\tau = -\kappa \cdot TEC/f^2$, where κ is a constant ($\approx$40.3 m^3Hz^2/el), f (in Hz) is the GNSS signal radio frequency, and one TEC unit is defined as TECU = 10^{16} el/m^2 $\approx 1.66 \times 10^{-8}$ mol/m^2. The ionospheric delay reaches the maximum (~4.8 m) at 12:00 LT on 8 September 2017.

We assume a space weather event like the 8–11 September 2017 one to occur in the future. We will study the elevated satellite-based positioning errors resulting from such a space weather event, and the consequent impact on the operational capacity at HKIA.

2.2. Scenario Assumptions

We are able to obtain the flight data during the 8–11 September 2017 geomagnetic storm. However, no data about aircraft final approach and landing failure caused by GNSS positioning errors are available to us. We will

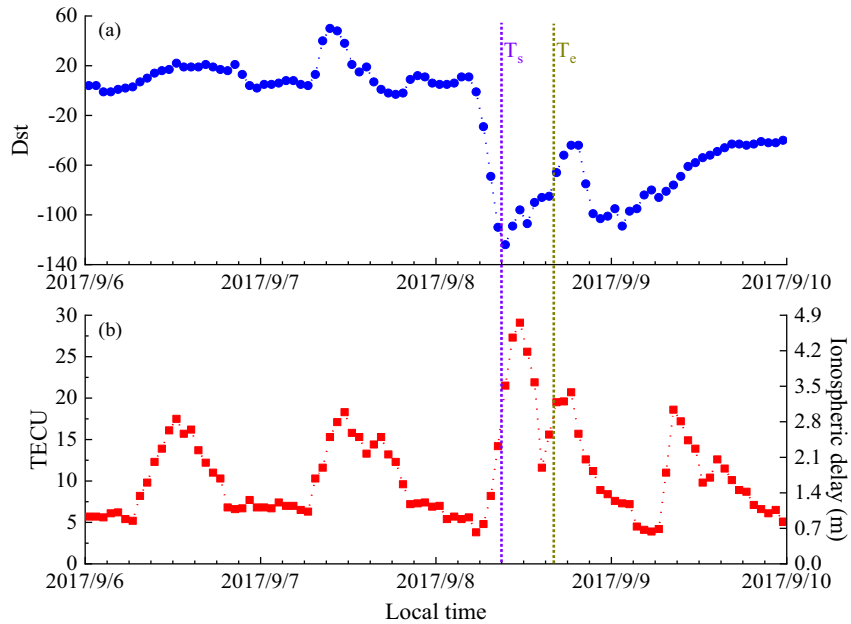

Figure 2. (a) The provisional Dst and (b) the total electron content variation and ionospheric delay in the Hong Kong area during an intense geomagnetic storm. The two vertical lines denote T_s = 09:00 LT and T_e = 16:00 LT on 8 September 2017.

base our study on a projection of the future flight demand at the HKIA, and the steps for simulating the future flight demand are as follows. The hourly arrival flight demand is first captured using flight data of the HKIA on 8 September 2019. Then, based on an annual growth rate of 5% in the Asia Pacific region for passenger air traffic from 2019 to 2040 (Mazareanu, 2021), the hourly arrival demand in 2030 is estimated. Considering the landing separation standards, the landing time of arrival flights are simulated together with other information, such as callsign, scheduled departure time, planned enroute time, scheduled landing time, etc. Figure 3 depicts the historical and predicted hourly arrival demand of the HKIA.

Currently, the airport acceptance rate (AAR), which is defined as the number of flights allowed to land at a given airport within 1 hr (Mukherjee et al., 2012), is 30, that is, 2-min arrival slot interval for a single-runway airport (ICAO, 2016). This is based on the ground navigation system such as the ILS. Considering the limitation of AAR based on ground navigation and booming flight demand, the ICAO introduced satellite navigation to boost airspace capacity and flight efficiency by lowering minimum separation standards. With satellite navigation, the AAR is assumed to be 60, 1-min arrival slot interval.

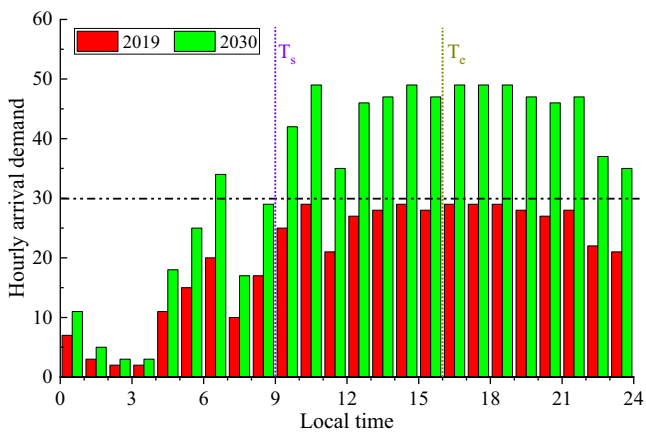

Figure 3. The red histograms denote the hourly arrival demand of the Hong Kong International Airport on 8 September 2019. The green histograms denote the predicted hourly arrival demand in the year 2030.

We assume that the ground navigation will be used to replace the satellite navigation during the final approach and landing phases between T_s = 09:00 and T_e = 16:00 LT during such a geomagnetic storm when the space weather impact is substantial. Thus, AAR will be reduced from 60 to 30 during the period T_s to T_e. Figure 3 shows that during peak hours, the estimated arrival demand exceeds 30 flights per hour, implying that some arrival flights may need to be rescheduled (including delay, cancellation, and diversion). The assumptions for the simulated scenario are summarized in Table 2. In our study, we also assume the departure flights from the airport will not be affected by space weather, since aircraft does not rely on GNSS navigation to take off.

2.3. ATM Rules During the Geomagnetic Storm

There will be an imbalance between arrival flight demands and airport capacity when the navigation mode switches from satellite navigation

Table 2
Summary of Key Assumptions

Index	Explanation
Arrival flight demand	Predicted arrival demand in green histograms of Figure 3
Airport arrival rate	60 per hour based on satellite navigation
Satellite navigation failure time	09:00–16:00 LT

(AAR = 60) to ground navigation (AAR = 30). Ground Delay Programs (Glover & Ball, 2013), which is a safe and cost-effective means of shifting predicted airborne delay to ground delay, is the most comprehensive traffic flow management strategy for solving such an imbalance problem. From the standpoint of fairness among different airlines, the arrival time for each flight is assigned in the ascending order of the original time of arrival (OTA) (Vossen & Ball, 2006), that is, flights having earlier OTAs receive an earlier controlled time of arrival (CTA) than flights with later OTAs. Figure 4 demonstrates the change of arrival flight schedule.

We design a revised ATM rule based on whether or not the ionospheric delay can be forecasted. This can also be interpreted as whether the duration of the satellite navigation failure can be forecasted or not.

Condition 1. Without Ionospheric Delay Forecast.
If we are unable to forecast the large ionospheric error caused by space weather events, air traffic controllers (ATCs) are informed only when the space weather event commences at T_s. The rescheduling rules are thus as follows.

(1) Flights with OTD/OTA (OTD: original time of departure) prior to T_s depart from their original airports and land at HKIA as scheduled.
(2) Because airborne flights have a higher priority of landing than the ones on the ground, ATCs assign CTA for each airborne flight in ascending order of their OTA considering the available landing slots. If the CTA minus the OTA for a specific airborne flight is longer than 40 min, this flight will be diverted to an alternate airport due to the fuel consumption constraint.
(3) ATCs will then assign the CTA (remaining landing time slots) to each flight on the ground in ascending order according to their OTA. If the difference between CTD (Controlled Time of Departure) and OTD for a specific flight on the ground is more than 100 min, this flight will be canceled, and the corresponding time slot will be available for other flights.
(4) At T_e, ATCs are informed that the AAR of HKIA recovers to 60, and then ATCs reschedule flights based on the updated information.

Condition 2. With Ionospheric Delay Forecast.
If we are able to forecast the ionospheric delay with a forecast lead time (FLT) of δ ($\delta \neq 0$, in the units of hours), ATCs will determine the flight arrivals ahead of the development of a space weather event, that is, at $(T_s - \delta)$ ATCs will be informed that the AAR will decrease to 30 starting from T_s. According to the availability of the common inputs of space weather forecast models and their computational capabilities, we assume four different specific cases with $\delta = 1, 2, 4$, and 24 hr, denoted as FLT1, FLT2, FLT4, and FLTL, respectively. Note that FLTL

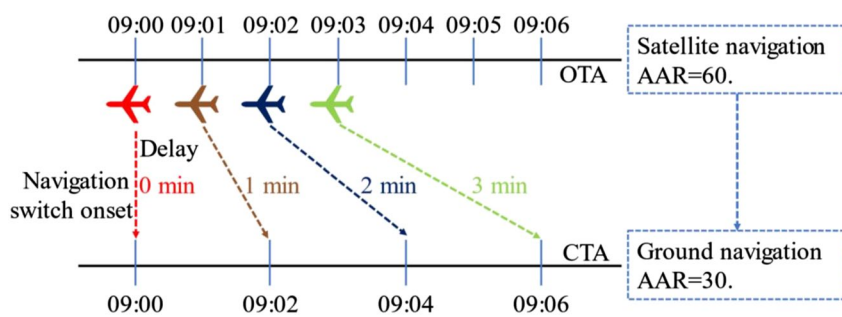

Figure 4. Switch from satellite-navigation-based arrival flight schedule (upper time axis: every 1 min) to ground-navigation-based arrival flight schedule (lower time axis: every 2 min).

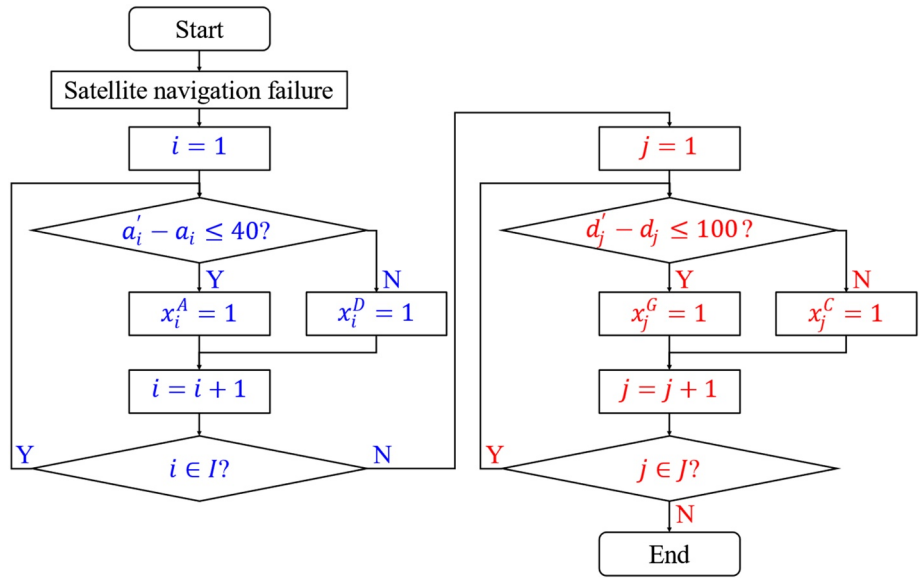

ATM rules

(1) Assignments for airborne flights

Callsign	OTA	CTA	Status	Delay
HDA485	13:46	13:46	$x_i^A = 1$	0 min
CPA503	14:13	14:14	$x_i^A = 1$	1 min

(2) Assignments for flights on the ground

Callsign	OTD	CTD	Status	Delay
AAR721	12:31	14:10	$x_j^G = 1$	99 min
KAL613	12:33	14:12	$x_j^G = 1$	99 min
JNA113	12:34	X	$x_j^C = 1$	0 min
KAL613	12:35	X	$x_j^C = 1$	0 min
EVA867	12:36	14:16	$x_j^G = 1$	100 min

Figure 5. Flowchart for the calculation of landing times in air traffic management (ATM; above) and results of calculation examples (below). Please note that the landing time 14:14 is not available in the second step of ATM rules (flights on the ground assignments), as this time (14:14) has already been assigned to the airborne flight CPA503 due to the landing priority of CPA503.

(with "L" denoting "long hours") represents the case with a 24-hr FLT. Lead time longer than 24 hr has not been considered as no civil flight flies longer than 24 hr. The rescheduling rules are as follows.

(1) Flights with OTD/OTA prior to $T_s - \delta$ depart from their original airports and land at HKIA as scheduled. ATCs will assign CTA for each airborne flight, whose OTA is later than T_s.

(2) to (3) are the same as described for Condition 1.

(4) At $(T_e - \delta)$, ATCs are informed that the AAR will recover to 60 from T_e, and ATCs will reschedule flights based on the updated information.

2.4. Solution Methodology for ATM

Let I be the set of airborne flights in the ascending order of their OTA indexed by i and let J be the set of flights on the ground in the ascending order of their OTA indexed by j. In the ATM rules, each airborne flight i may be assigned some airborne delays ($x_i^A = 1$) or divert to land at an alternate airport ($x_i^D = 1$). Similarly, each flight j on the ground may be assigned some ground delays ($x_j^G = 1$) or be canceled ($x_j^C = 1$). Just as shown in Figure 5, the

Table 3
Defined Notations and Explanations

Notation	Explanation
I	Set of airborne flights in the ascending order of their OTA (indexed by i)
J	Set of flights on the ground in the ascending order of their OTA (indexed by j)
a_i	The original time of arrival of airborne flight i
a_i'	The control time of arrival of airborne flight i
a_j	The original time of arrival of flight j on the ground
a_j'	The control time of arrival of flight j on the ground
d_j	The original time of departure of flight j on the ground
d_j'	The control time of departure of flight j on the ground
L_j	The enroute flight time of flight j, $L_j = a_j - d_j = a_j' - d_j'$
T_j^G	Ground delay time (in the units of minutes), $T_j^G = d_j' - d_j$
T_i^A	Airborne delay time (in the units of minutes), $T_i^A = a_i' - a_i$
W_C	The average cost of a canceled flight
W_D	The average cost of a diverted flight
W_G	The average cost of ground delay per minute
W_A	The average cost of airborne delay per minute
x_i^A	$x_i^A = 1$, if $T_i^A \le 40$; $x_i^A = 0$, otherwise
x_i^D	$x_i^D = 1$, if $T_i^A > 40$; $x_i^D = 0$, otherwise
x_j^G	$x_j^G = 1$, if $T_j^G \le 100$; $x_j^G = 0$, otherwise
x_j^C	$x_j^C = 1$, if $T_j^G > 100$; $x_j^C = 0$, otherwise

detailed steps of solution methodology for ATM during space weather are presented. When satellite navigation is out of work and AAR reduces from 60 to 30, the assignments for these airborne flights will be conducted first because airborne fights receive a priority of landing. For each airborne flight i, the OTA and CTA are denoted by a_i and a_i', respectively. If the assigned airborne delay time $T_i^A = a_i' - a_i \le 40$, this flight i will accept the assigned airborne delay and will land at the HKIA at a_i', $\Longrightarrow x_i^A = 1$; otherwise, that is, $T_i^A > 40$, flight i will land at an alternate airport without any airborne delay, $\Longrightarrow x_i^D = 1$.

After giving directions to airborne flights, the assignments for flights on the ground will then be carried out. For each flight j on the ground, the OTA, CTA, OTD, and CTD are denoted as a_j, a_j', d_j, and d_j', respectively. ATCs would assign a_j' to each flight j on the ground using the rest of available arrival time slots. Assuming that the enroute flight time L_j is known and deterministic, the CTD can be calculated by $d_j' = a_j' - L_j$ and the assigned ground delay is $T_j^G = d_j' - d_j$. If $T_j^G \le 100$, this flight j will accept the assigned ground delay and will depart from the origin airport at d_j', $\Longrightarrow x_j^G = 1$; otherwise, that is, $T_j^G > 100$, flight j will be canceled without any ground delay, $\Longrightarrow x_j^C = 1$.

Given the notations listed in Table 3, the total airborne delay time is $\sum_{i\in I} x_i^A T_i^A$; the number of diverted flights is $\sum_{i\in I} x_i^D$; the total ground delay time is $\sum_{j\in J} x_j^G T_j^G$; the number of canceled flights is $\sum_{j\in J} x_j^C$. Thus, the financial costs related to airlines induced by space weather can be expressed in Equation 1:

$$\text{Cost} = \sum_{i\in I}\left(W_A x_i^A T_i^A + W_D x_i^D\right) + \sum_{j\in J}\left(W_G x_j^G T_j^G + W_C x_j^C\right) \tag{1}$$

s.t.

$$T_j^G = d_j' - d_j \tag{2}$$

$$T_i^A = a_i' - a_i \tag{3}$$

$$x_i^A + x_i^D + x_j^G + x_j^C = 1 \tag{4}$$

$$x_i^D = 1 | T_i^D > 40 \tag{5}$$

$$x_i^A = 1 | T_i^D \leq 40 \tag{6}$$

$$x_i^D + x_i^A = 1 \tag{7}$$

$$x_j^C = 1 | T_j^G > 100 \tag{8}$$

$$x_j^G = 1 | T_j^G \leq 100 \tag{9}$$

$$x_j^C + x_j^G = 1 \tag{10}$$

The ground delay and airborne delay can be calculated by Equations 2 and 3, respectively. Equation 4 ensures that each flight can only have one assignment case. Equations 5 and 6 illustrate the conditions of diverted flights and airborne delay flights. For each airborne flight i, it may be a diverted flight ($x_i^D = 1$) or an airborne delay flight ($x_i^A = 1$), expressed in Equation 7. Similarly, Equations 8 and 9 illustrate the conditions of canceled flights and ground delay flights. For each flight j on the ground, it may be a canceled flight ($x_j^C = 1$) or a ground delay flight ($x_j^G = 1$), expressed in Equation 10.

3. Results and Discussions

3.1. Impact of Forecast Lead Times

Figure 6a shows the simulated landing time of each flight for various FLTs based on the above-defined ATM rules. Although the satellite navigation failure duration is from 09:00 LT to 16:00 LT, the recovery time is actually after 22:00 LT, demonstrating the long-time effect of space weather. In theory, the CTA of a specific flight would have more delay if the FLT is shorter. This is because air traffic would be more jammed when space weather information is obtained with a shorter lead time. In addition, flights with OTA before ($T_s - \delta$) would depart from their original airports as scheduled. Therefore there would be more flights taking off if the FLT δ is shorter, causing more airborne delays. A trend of longer airborne delay can be seen at the beginning of the peak hour (Figure 6b), with simulated flights in FLT0 scenario generally experiencing the longest delays, followed by flights in FLT1, FLT2, FLT4, and FLTL scenarios. FLT0 denotes the scenario in Condition 1, that is, no forecast. Herein, we did not calculate the results under FLT3. Such a trend is more remarkable in Figure 6c when the delay effects are accumulating. The simulated CTA distribution is more complicated than the ideal case, considering that different flights have different origins and thus different enroute times. Figure 6b illustrates that the number of canceled flights decreases as FLT grows. The canceled flights predominantly cluster during peak hours (13:00–15:00 LT). This is because the assigned ground delay for each flight starts to accumulate after 09:00 LT. A substantial number of flights are delayed on the ground for more than 100 min during peak hours, which will be canceled. If ATCs are unable to get information on the upcoming space weather, they prefer to cancel flights. Note that a few flights are canceled before 11:00 LT under scenarios FLT0 and FLT1. Some flights still on the ground with short enroute time can also be delayed or canceled. This is a result of a substantially reduced number of available landing slots because landing intervals are increased from 1 min to 2 min, and airborne flights receive a priority of landing.

3.2. Cost Estimation Under Different Forecast Lead Times

The direct costs related to airlines resulting from the space weather event due to flight delays, cancellations, and diversions are also estimated. The average cost of flight cancellation is W_C = €18,570; the average cost of flight diversion is W_D = €7,800; the average cost of ground delay is W_G = €16/min; and the average cost of airborne delay is W_A = €74/min (EUROCONTROL, 2020). Figure 7 shows the impact of different FLTs on flight

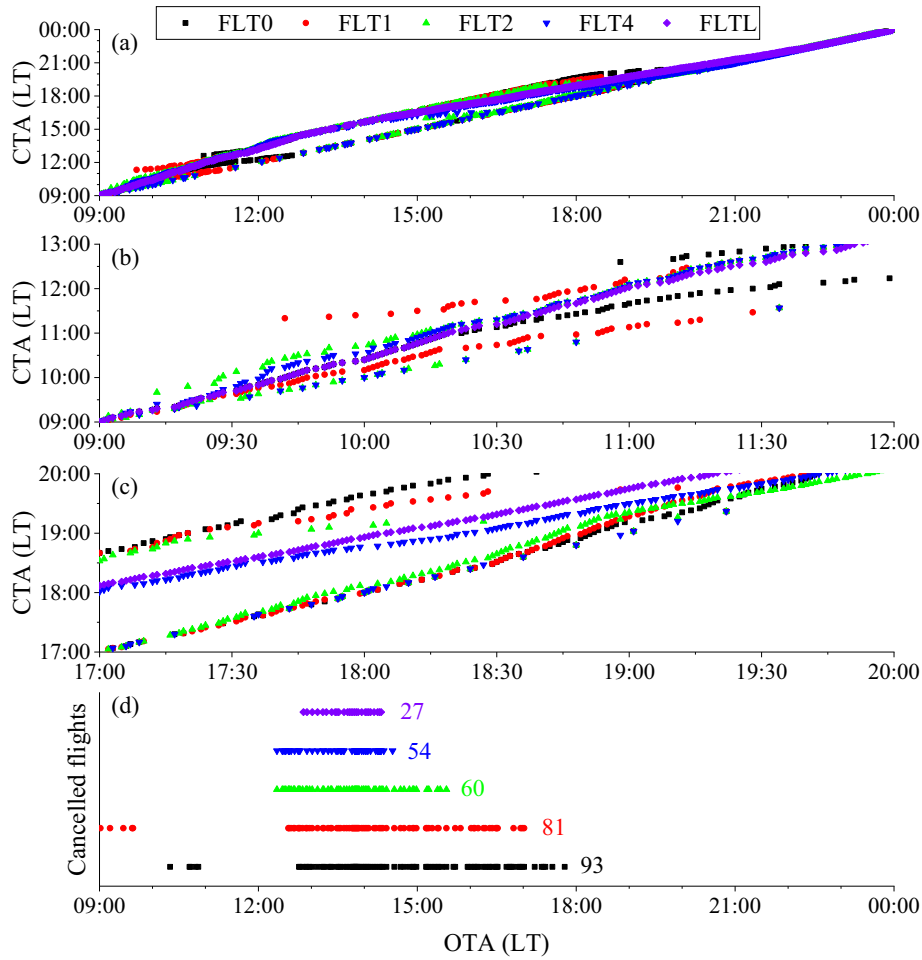

Figure 6. (a) The Controlled Time of Arrival (CTA) under different forecast scenarios. Each dot represents one flight. (b) The detailed CTA distribution at the beginning of space weather. (c) The detailed CTA distribution after space weather. (d) The distribution of the total number of canceled flights versus original time of arrival.

assignments and extra financial costs related to airlines. As indicated in Figure 7a, with the increase of FLT, the airborne delays drop dramatically from 2,558 min (FLT0) to 0 min (FLTL); while the ground delays increase dramatically from 17,324 min (FLT0) to 31,950 min (FLTL). Ground delay is defined as the difference between the CTD and OTD for a grounded flight and airborne delay is defined as the difference between the CTA and OTA for an airborne flight. Because ATCs have enough time to make decisions under scenario FLTL, flights will be rescheduled well ahead of the occurrence of the space weather event and thus they are delayed on the ground. However, without forecast (FLT0), significant air traffic congestion will result in massive airborne delays. In addition, if there is no forecast (FLT0), five diverted flights will land at other alternate airports near Hong Kong. This is due to the fact that more flights will depart from their origin airports before T_s in the case of no forecast FLT0, compared to the case with a forecast, which increases the possibility of flight diversion. In our simulation, there is no flight diversion under other forecast scenarios because there are not too many flights in the air during this event. Figure 7b indicates that as forecast capabilities improve, the number of canceled flights decreases. ATCs have less confidence in the future AAR when the FLT is shorter. Therefore, they prefer to cancel flights to avoid unexpected problems like airborne holding or flight diversions. If a flight is canceled, there will be no ground delay for this flight, and the time slot associated with this flight can be utilized by other planes. This also helps to explain why, in Figure 7a, the overall ground delays are lower when the FLT is smaller. Figure 7c shows that without space weather forecasting the extra financial cost related to airlines is 2.23 million Euros and that the cost decreases as the FLT grows.

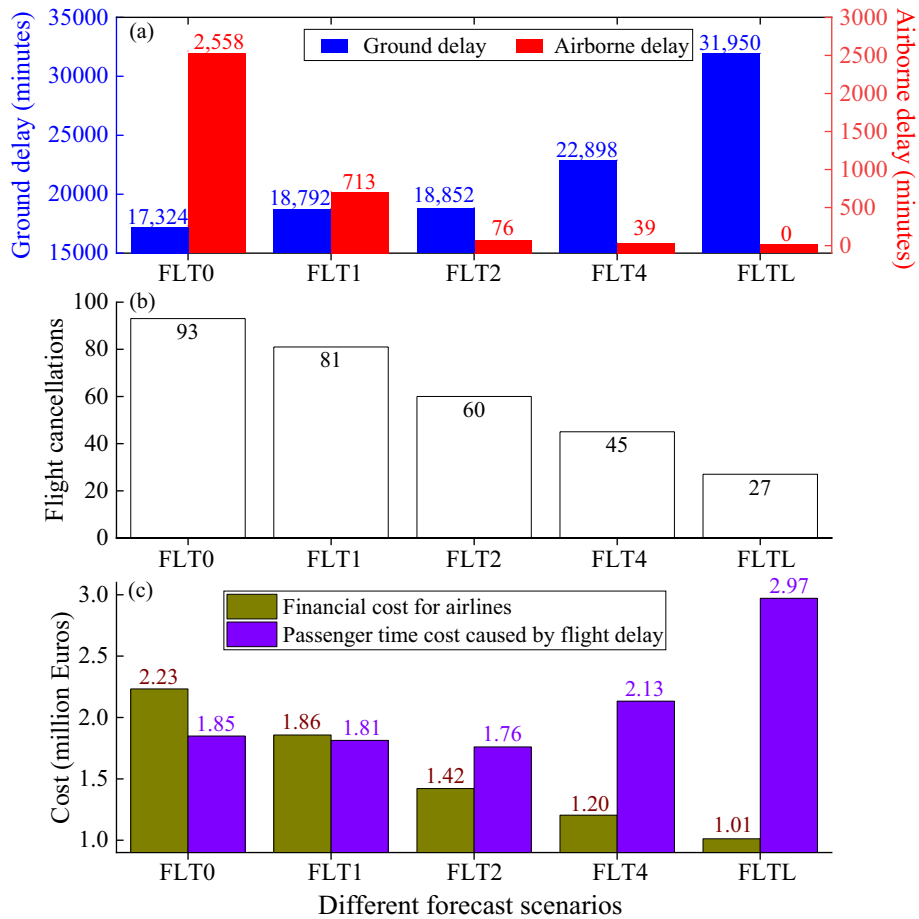

Figure 7. The impact of different forecast scenarios on (a) the total ground delay time and total airborne delay time, (b) the number of flight cancellations, and (c) extra financial costs for airlines and flight-delay-caused passenger time costs.

In addition, the cost associated with the time delay for each passenger is estimated to be about €35.0/hr (Ball et al., 2010). Hence, assuming 200 seats in a typical B757 configuration with an occupancy factor of 80%, the unit delay cost for all passengers is $200 \times 80\% \times 35.0/60 = 93$ €/*min*. Based on the ground delay time and airborne delay time in Figure 7a, the passenger delay cost can be 1.85 million Euros (FLT0), 1.81 million Euros (FLT1), 1.76 million Euros (FLT2), 2.13 million Euros (FLT4), and 2.97 million Euros (FLTL) (shown in Figure 7c). On an aggregate basis, the adverse effects of flight delays can be various such as reducing passenger demand and destroying airline scheduling plans (Britto et al., 2012), which may introduce additional indirect economical loss and affect the aggregate economy.

Table 4
Comparison of the Impact of the Accuracy of the Forecast

	Optimistic forecast: 09:00–14:00	Pessimistic forecast: 09:00–18:00	Accurate forecast: 09:00–16:00
Ground delay (min)	12,739	38,000	31,950
Airborne delay (min)	4,184	0	0
No. of canceled flights	56	60	27
No. of diverted flights	38	0	0
Cost for airlines (million Euros)	1.85	1.72	1.01

3.3. Impact of the Accuracy of Space Weather Forecast

We also investigate how forecast accuracy affects ATM by simulating two more scenarios. In the optimistic forecast, we assume that the adverse event would end 2 hr earlier than it actually does, that is, T_s = 09:00 and T_e = 14:00. In the pessimistic forecast, we assume that an adverse event would end 2 hr later than it actually does, that is, T_s = 09:00 and T_e = 18:00. We also assume the forecast capabilities are set to FLTL. As shown in Table 4, the optimistic forecast results in much fewer ground delays than the accurate forecast, but significantly more airborne delays, flight cancellation, and diversion. The induced cost for airlines (1.85 million Euros) is about 83% more than the accurate forecast (1.01 million Euros). Because more flights will be

optimistically scheduled to be in the air if the space weather event is expected to end earlier than it actually does, generating traffic congestion and hence flight diversion. On the other hand, the pessimistic forecast results in more ground delays and more flight cancellations than the accurate forecast. The induced cost (1.72 million Euros) is 70% more than the accurate forecast. If the space weather event is predicted to linger longer than it does, more flights will be grounded pessimistically. The findings show that reliable forecasting is crucial for ATM and cost savings. It also implies that an optimistic forecast has a more harmful impact than a pessimistic forecast. The cost resulting from an optimistic forecast is 1.08 times of that from a pessimistic forecast.

4. Conclusions

Space weather can significantly change the ionosphere conditions, which can result in an impact on satellite-based aircraft operations. This study focuses on the analysis of the impact of a hypothesized space weather scenario on HKIA, a typical location in the equatorial ionospheric anomaly region. Based on the data from a relatively minor space weather event during 8–11 September 2017, the effects of GNSS positioning errors induced by the space weather on satellite-based ATM are estimated. In the case of adverse GNSS positioning errors, ATM rules are designed to handle the capacity-demand imbalance problem. Three flight performance indices namely canceled flights, diverted flights, and flight delays are used to examine the impact of space weather on ATM. In the analysis, the factors such as distribution of arrival flight demand, the duration of satellite navigation failures, and space weather forecast capabilities, have been considered. Our simulation results suggest that if the ionospheric impact on GNSS navigation cannot be predicted, the cost related to airlines incurred to arrival flights at HKIA would be more than 2 million Euros. This cost is reduced to 1 million Euros if the ionospheric impact is precisely predicted. In addition, the time costs for passengers caused by flight delays can reach nearly 3 million Euros. We also show that the cost of an optimistic forecast and a pessimistic forecast is 1.83 times and 1.70 times of an accurate forecast, respectively. The cost related to airlines reduces as FLT increases. Considering flight time for a certain flight plan of less than 24 hr and daily flight planning, the FLT at least 24 hr can satisfy the requirement of pre-tactical ATM. Improving the accuracy and extending the lead time of ionospheric impact forecast on GNSS navigation are crucially important for the aviation industry to reduce impacts and costs during space weather events.

Data Availability Statement

The authors thank Opensky for providing the flight data, publicly accessible at https://opensky-network.org/. The Dst index was obtained from https://omniweb.gsfc.nasa.gov/form/dx1.html and the total electron content data was obtained from https://cddis.nasa.gov/archive/gnss/products/ionex/.

Acknowledgments
This work was supported by the Hong Kong Research Grants Council (RGC) projects (Q80Q RGC/Gov No. PolyU 15221620), the Emerging Frontier Area (EFA) Scheme of Research Institute for Sustainable Urban Development (RISUD) of the Hong Kong Polytechnic University under Grant 1-BBWJ, and the Stable Support Plan Program of Shenzhen Natural Science Fund (Grant No. 20200925153644003). The project support (ZVVC-ZVN6) from the Hong Kong Polytechnic University is also appreciated.

References

Astafyeva, E., Yasyukevich, Y., Maksikov, A., & Zhivetiev, I. (2014). Geomagnetic storms, super-storms, and their impacts on GPS-based navigation systems. *Space Weather*, *12*(7), 508–525. https://doi.org/10.1002/2014SW001072

Ball, M., Barnhart, C., Dresner, M., Hansen, M., Neels, K., Odoni, A., et al. (2010). *Total delay impact study*. NEXTOR Research Symposium. Retrieved from https://isr.umd.edu/NEXTOR/pubs/TDI_Report_Final_11_03_10.pdf

Blanch, J., Walter, T., & Enge, P. (2012). Satellite navigation for aviation in 2025. *Proceedings of the IEEE*, *100*(Special Centennial Issue), 1821–1830. https://doi.org/10.1109/JPROC.2012.2190154

Britto, R., Dresner, M., & Voltes, A. (2012). The impact of flight delays on passenger demand and societal welfare. *Transportation Research Part E: Logistics and Transportation Review*, *48*(2), 460–469. https://doi.org/10.1016/j.tre.2011.10.009

Bubalo, B., & Gaggero, A. A. (2021). Flight delays in European airline networks. *Research in Transportation Business & Management*, *41*, 100631. https://doi.org/10.1016/j.rtbm.2021.100631

Cerruti, A. P., Kintner, P. M., Jr., Gary, D. E., Mannucci, A. J., Meyer, R. F., Doherty, P., & Coster, A. J. (2008). Effect of intense December 2006 solar radio bursts on GPS receivers. *Space Weather*, *6*(10), S10D07. https://doi.org/10.1029/2007SW000375

Cesaroni, C., Spogli, L., Aragon-Angel, A., Fiocca, M., Dear, V., De Franceschi, G., & Romano, V. (2020). Neural network based model for global Total Electron Content forecasting. *Journal of Space Weather and Space Climate*, *10*, 11. https://doi.org/10.1051/swsc/2020013

Coster, A. J., & Yizengaw, E. (2021). *GNSS/GPS degradation from space weather* (pp. 165–181). Space Weather Effects and Applications. https://doi.org/10.1002/9781119815570.ch8

Dubey, S., Wahi, R., & Gwal, A. (2006). Ionospheric effects on GPS positioning. *Advances in Space Research*, *38*(11), 2478–2484. https://doi.org/10.1016/j.asr.2005.07.030

Enge, P., Enge, N., Walter, T., & Eldredge, L. (2015). Aviation benefits from satellite navigation. *New Space*, *3*(1), 19–35. https://doi.org/10.1089/space.2014.0011

EUROCONTROL. (2020). *EUROCONTROL standard inputs for economic analyses*. Retrieved from https://www.eurocontrol.int/publication/eurocontrol-standard-inputs-economic-analyses

Glover, C. N., & Ball, M. O. (2013). Stochastic optimization models for ground delay program planning with equity–efficiency tradeoffs. *Transportation Research Part C: Emerging Technologies*, *33*, 196–202. https://doi.org/10.1016/j.trc.2011.11.013

Guo, J., & Geng, J. (2018). GPS satellite clock determination in case of inter-frequency clock biases for triple-frequency precise point positioning. *Journal of Geodesy*, *92*(10), 1133–1142. https://doi.org/10.1007/s00190-017-1106-y

Hoque, M. M., & Jakowski, N. (2011). Ionospheric bending correction for GNSS radio occultation signals. *Radio Science*, *46*(06), 1–9. https://doi.org/10.1029/2010RS004583

Huang, Z., & Yuan, H. (2013). Analysis and improvement of ionospheric thin shell model used in SBAS for China region. *Advances in Space Research*, *51*(11), 2035–2042. https://doi.org/10.1016/j.asr.2012.12.018

ICAO. (2016). Doc 4444–Procedures for air navigation services: Air traffic management. In *International aviation civil organization Montreal*. Retrieved from https://ops.group/blog/wp-content/uploads/2017/03/ICAO-Doc4444-Pans-Atm-16thEdition-2016-OPSGROUP.pdf

Kim, E., & Choi, D. (2016). A UWB positioning network enabling unmanned aircraft systems auto land. *Aerospace Science and Technology*, *58*, 418–426. https://doi.org/10.1016/j.ast.2016.09.005

Kim, J., Kim, Y., Song, J., Kim, D., Park, M., & Kee, C. (2019). Performance improvement of time-differenced carrier phase measurement-based integrated GPS/INS considering noise correlation. *Sensors*, *19*(14), 3084. https://doi.org/10.3390/s19143084

Lee, J., Pullen, S., Datta-Barua, S., & Lee, J. (2016). Real-time ionospheric threat adaptation using a space weather prediction for GNSS-based aircraft landing systems. *IEEE Transactions on Intelligent Transportation Systems*, *18*(7), 1752–1761. https://doi.org/10.1109/TITS.2016.2627600

Lin, C.-H., Liu, J.-Y., Tsai, H.-F., & Cheng, C.-Z. (2007). Variations in the equatorial ionization anomaly peaks in the Western Pacific region during the geomagnetic storms of April 6 and July 15, 2000. *Earth Planets and Space*, *59*(5), 401–405. https://doi.org/10.1186/BF03352701

Linty, N., Minetto, A., Dovis, F., & Spogli, L. (2018). Effects of phase scintillation on the GNSS positioning error during the September 2017 storm at Svalbard. *Space Weather*, *16*(9), 1317–1329. https://doi.org/10.1029/2018SW001940

Mazareanu, E. (2021). *Air traffic – Passenger growth rates forecast 2019–2040*. Retrieved from https://www.statista.com/statistics/269919/growth-rates-for-passenger-and-cargo-air-traffic/

Moreno, B., Radicella, S., De Lacy, M., Herraiz, M., & Rodriguez-Caderot, G. (2011). On the effects of the ionospheric disturbances on precise point positioning at equatorial latitudes. *GPS Solutions*, *15*(4), 381–390. https://doi.org/10.1007/s10291-010-0197-1

Mukherjee, A., Hansen, M., & Grabbe, S. (2012). Ground delay program planning under uncertainty in airport capacity. *Transportation Planning and Technology*, *35*(6), 611–628. https://doi.org/10.1080/03081060.2012.710031

National Research Council. (2008). *Severe space weather events: Understanding societal and economic impacts: A workshop report*. The National Academies Press. https://doi.org/10.17226/12507

Pejovic, T., Noland, R. B., Williams, V., & Toumi, R. (2009). A tentative analysis of the impacts of an airport closure. *Journal of Air Transport Management*, *15*(5), 241–248. https://doi.org/10.1016/j.jairtraman.2009.02.004

Phoomchusak, P., Leelaruji, N., & Hemmakorn, N. (2013). The deterioration of GPS accuracy caused by ionospheric amplitude scintillation. In *Citeseer*. Retrieved from http://citeseerx.ist.psu.edu/viewdoc/summary?doi=10.1.1.518.6058

Sharma, R., & Hablani, H. (2014). High-accuracy GPS-based aircraft navigation for landing using pseudolites and double-difference carrier phase measurements. *IFAC Proceedings Volumes*, *47*(1), 200–204. https://doi.org/10.3182/20140313-3-IN-3024.00224

Sun, R., Hsu, L.-T., Xue, D., Zhang, G., & Ochieng, W. Y. (2019). GPS signal reception classification using adaptive neuro-fuzzy inference system. *Journal of Navigation*, *72*(3), 685–701. https://doi.org/10.1017/S0373463318000899

Tsagouri, I., Koutroumbas, K., & Elias, P. (2018). A new short-term forecasting model for the total electron content storm time disturbances. *Journal of Space Weather and Space Climate*, *8*, A33. https://doi.org/10.1051/swsc/2018019

Tsurutani, B., Mannucci, A., Iijima, B., Abdu, M. A., Sobral, J. H. A., Gonzalez, W., et al. (2004). Global dayside ionospheric uplift and enhancement associated with interplanetary electric fields. *Journal of Geophysical Research*, *109*(A8), A08302. https://doi.org/10.1029/2003JA010342

Vismari, L. F., & Junior, J. B. C. (2011). A safety assessment methodology applied to CNS/ATM-based air traffic control system. *Reliability Engineering & System Safety*, *96*(7), 727–738. https://doi.org/10.1016/j.ress.2011.02.007

Vossen, T., & Ball, M. (2006). Optimization and mediated bartering models for ground delay programs. *Naval Research Logistics*, *53*(1), 75–90. https://doi.org/10.1002/nav.20123

Xue, D., Hsu, L.-T., Wu, C.-L., Lee, C.-H., & Ng, K. K. (2021). Cooperative surveillance systems and digital-technology enabler for a real-time standard terminal arrival schedule displacement. *Advanced Engineering Informatics*, *50*, 101402. https://doi.org/10.1016/j.aei.2021.101402

Yu, S., & Liu, Z. (2021a). Feasibility analysis of GNSS-based ionospheric observation on a fast-moving train platform (GIFT). *Satellite Navigation*, *2*(1), 1–18. https://doi.org/10.1186/s43020-021-00051-1

Yu, S., & Liu, Z. (2021b). The ionospheric condition and GPS positioning performance during the 2013 tropical cyclone Usagi event in the Hong Kong region. *Earth Planets and Space*, *73*(1), 1–16. https://doi.org/10.1186/s40623-021-01388-2

Zhang, S., Du, S., Li, W., & Wang, G. (2019). Evaluation of the GPS precise orbit and clock corrections from MADOCA real-time products. *Sensors*, *19*(11), 2580. https://doi.org/10.3390/s19112580

Ziv, S. Z., Yair, Y., Alpert, P., Uzan, L., & Reuveni, Y. (2021). The diurnal variability of precipitable water vapor derived from GPS tropospheric path delays over the Eastern Mediterranean. *Atmospheric Research*, *249*, 105307. https://doi.org/10.1016/j.atmosres.2020.105307